Comparison of Computed Torque and Sliding Mode Trajectory Tracking of a Human-like Walking Trajectory for a 2-Dimensional Biped Walker with Knees

Felipe C. R. Miftajov

Abstract— **Underactuation is desirable in walking robots but increases difficulty of control. This paper compares the performance of a computed torque method (CMT) controller and a sliding mode control (SMC) controller in the tracking of a human-like walking trajectory for a fully actuated biped robot with knees. Results are given for progressively decreasing ankle torque limits to demonstrate the poor performance of the controllers in an underactuated robot; the controllers are also compared under parameter uncertainty to compare their robustness.**

I. INTRODUCTION

Achieving stable, human-like walking in biped robots is a challenging problem. Underactuation in robots is a desirable goal because it tends to make them more energy efficient; in addition, human walking is inherently underactuated [1]. However, underactuation makes the control problem even more challenging since some of the joints cannot be directly controlled, and have to be stabilized using the zero dynamics or hybrid dynamics of the system [1]. This paper will analyze a fully actuated biped walker while showing some of the issues that occur if a controller developed for a fully actuated robot is applied to an underactuated system.

This paper will focus on a 2-dimensional biped with actuated knees and hips, and rigid circular feet, inspired by McGeer's early passive walker design [2] and Hsu's walker with knees and point feet [3]. This system is modeled by McGeer as an open chain of 4 rigid links with arbitrary dimensions and mass properties, with the ability to roll about the first link; the nonlinear dynamics equations derived in his paper [2] will be implemented in MATLAB along with impact calculations that allow multiple steps to be simulated. Then, using Matthew Kelly's trajectory optimization library for MATLAB [4], a human-like trajectory will be generated by numerically solving an optimization problem to minimize the norm of the Lagrangian of the system. The resulting joint trajectories will be approximated by 10th order polynomials, which are differentiated to find the desired angular velocities and accelerations.

The controllers considered in this paper are computed torque method (CTM) control and sliding mode control (SMC). The computed torque method is a direct extension of feedback linearization and is commonly used in fully actuated robotics [5]. A CTM controller be implemented to track this trajectory with a fully actuated biped. The computed torque controller is simple to implement but limited in application if not all the joints can be controlled [6]. The torque provided by the ankle will be gradually limited to illustrate the limits of control strategies developed for the fully actuated robot when applied to an underactuated robot.

Sliding mode control is a robust control strategy that can handle more disturbances, including parameter uncertainties, by its switching action [6]. SMC has been used in underactuated two degree-of-freedom (2-DOF) robots [7], [8] and even in a Free-link walking robot [9], but applying it to a system with more than two degrees of freedom is complex and will be discussed in a future paper. An integral sliding mode controller based on the one described by S. Moosavian et al. [6] will be implemented and applied to the fully actuated model, with limited ankle torque.

Finally, the performance of both controllers will be compared to evaluate their robustness to limiting the ankle torque and to model uncertainty. The metrics will be number of consecutive steps succesfully taken, the maximum torque input and tracking error over up to four steps, and considerations such as amount of chatter in the torque input.

II. MODEL AND TRAJECTORY GENERATION

A. Passive Walker Model and Actuation

The biped dynamics are derived almost exactly as in McGeer's derivation of the dynamics of an N-link chain [2, Appendix A], in the particular case of $N = 4$ and with the slope of the ground $\gamma = 0$. The derivation consists of subtracting the rate of change of angular momentum for consecutive joints. The resulting equation is somewhat modified from [2, eqs. (46) and (64)] to match robotics conventions:

$$\dot{H} = M(q)\ddot{q} + C(q,\dot{q})\dot{q} + G(q) = 0 \tag{1}$$

$$\dot{H} = \begin{bmatrix} \dot{H}_1 - \dot{H}2 \\ \dot{H}_2 - \dot{H}3 \\ \dot{H}_3 - \dot{H}4 \\ \dot{H}_4 \end{bmatrix}$$

$$-G = \begin{bmatrix} T_{g1} - T_{g2} \\ T_{g2} - T_{g3} \\ T_{g3} - T_{g4} \\ T_{g4} \end{bmatrix}$$

In (1), q is the vector of absolute joint angles (measured clockwise from vertical), $\dot{H}_i$ is the instantaneous rate of change of angular momentum about the i-th joint, and T_{gi} is the torque at the i-th joint due to gravity. M is symmetric and positive definite for all states of the system.

It is important to note that the subtraction process of the derivation means that any torque inputs to the equation τ_i must be expressed as differences of the physical joint torques T_i, as described by the transformation

$$\tau = \Phi T \tag{2}$$
$$\Phi = \begin{bmatrix} 1 & -1 & 0 & 0 \\ 0 & 1 & -1 & 0 \\ 0 & 0 & 1 & -1 \\ 0 & 0 & 0 & 1 \end{bmatrix}.$$

The bipedal walker is designed with no actuation at the ankles, so that only the knees and hip joint can be moved. However, this preliminary analysis will consider a fully actuated robot for simplicity and attempt to approximate underactuation by progressively decreasing the avaiable torque at the ankles.

The final system dynamics including input torques are described by

$$M\ddot{q} + C\ \mathrm{diag}(\dot{q})\dot{q} + G = \tau \tag{3}$$

These dynamics describe only the portions of the walk cycle in between foot impacts. To simplify analysis, it is assumed that only one foot (the stance foot) touches the ground during walking and that the transfer of weight from one foot to another happens instantaneously with the controller disabled.

The impact calculations assume an inelastic collision, with an impulse at the instant the swing foot collides with the ground. In the following equation, J is the Jacobian of the robot, F is the impact force, $\dot{q}_+$ are the joint velocities after impact, and $\dot{q}_+$ are the joint velocities before impact:

$$\begin{bmatrix} M & -J^\top \\ J & 0 \end{bmatrix} \begin{bmatrix} \dot{q}_+ \\ F \end{bmatrix} = \begin{bmatrix} M\dot{q}_- \\ 0 \end{bmatrix} \tag{4}$$

At impact, there is also a relabeling of the joints, common in walking analysis [2]. The new joint vector q_p is found by subtracting pi from each of the old joint angles and reversing their order:

$$q_p = \begin{bmatrix} 0 & 0 & 0 & 1 \\ 0 & 0 & 1 & 0 \\ 0 & 1 & 0 & 0 \\ 1 & 0 & 0 & 0 \end{bmatrix} \begin{bmatrix} q_1 - \pi \\ q_2 - \pi \\ q_3 - \pi \\ q_4 - \pi \end{bmatrix} \tag{5}$$

The new joint velocities are relabeled in a similar manner.

The mass and dimension parameters used for numerical analysis of the system are chosen to be average human values from biomechanics tables [10], [11].

B. Trajectory Generation by Optimization

A human-like walking trajectory is generated for the biped by solving an optimization problem that seeks an efficient gait that looks realistic:

$$\begin{aligned} \underset{t_F,\ q_d(t)}{\text{minimize}} \quad & \int_0^{t_F} ||L(t)||^2 dt \\ \text{subject to} \quad & C_e(q) = 0 \\ & C_i(q) \leq 0 \end{aligned} \tag{6}$$

where $q_d(t)$ is the desired trajectory for the joint angles, t_f is the duration of a step, L is the Lagrangian of the robot, and C_e and C_i are sets of equality and inequality constraints. These ensure that the step is identical for both legs, that the initial conditions match the next step's initial conditions to make the cycle periodic, that the knees never bend in the wrong direction, and that the swing foot does not touch the ground except at the beginning and end of a step.

This problem is solved with Matthew Kelly's OptimTraj library for MATLAB [4], using Hermite-Simpson direct collocation, where the trajectory is approximated using polynomial sections [12]. The solver returns a grid of time and trajectory values, which are then approximated by polynomials of order 10 so that the trajectory and its derivatives can be calculated at any point in time. Fig. 1 shows a walking tile that illustrates the obtained gait.

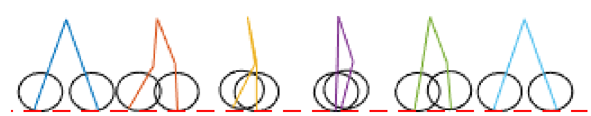

Fig. 1. Desired walking trajectory for the biped robot. Each location further to the right represents a later moment in time.

III. CONTROL

For the controls in this section, it is assumed that the position and velocity of all the joints are known, as they can easily be measured using encoders, tachometers, inertial measurement units (IMUs), etc.

A. Computed Torque Method

The computed torque method (CTM) controller assumes that the dynamics of the system are known exactly. Using the fact that the inertia matrix M is positive definite and therefore invertible, (3) can be rewritten as

$$\ddot{q} = M^{-1}(-C\dot{q} - G + \tau) \tag{7}$$

and then linearized by choosing

$$\tau = -\hat{C}\dot{q} - \hat{G} + \hat{M}\ddot{q}_r \tag{8}$$

where $\hat{M}, \hat{C}$, and $\hat{G}$ are the controller estimates of the corresponding parts of the system dynamics. Then, since the estimates are assumed to be exact, the new dynamics equation becomes

$$\ddot{q} = \ddot{q}_r \tag{9}$$

and the reference acceleration $\ddot{q}_r$ can be chosen to stabilize the desired trajectory.

Define $\tilde{q} = q - q_d$; then, one option is a PD controller:

$$\ddot{q}_r = \ddot{q}_d - K_d\dot{\tilde{q}} - K_p\tilde{q} \tag{10}$$

If K_d and K_p are diagonal matrices, this decouples the dynamics into second order scalar systems that can be made stable by choosing $K_d = 2 \cdot \mathrm{diag}(\omega_{n,i}),\ K_p = \mathrm{diag}(\omega_{n,i}^2)$ for $\omega_{n,i} > 0$:

$$\ddot{\tilde{q}} + K_d \dot{\tilde{q}} + K_p \tilde{q} = 0 \tag{11}$$

For the simulation, the natural frequency was chosen to be $omega_n = 40$ rad/s for all four joints. This was chosen by gradually decreasing the frequency to just above the point where the simulated robot could no longer walk four complete steps.

Since the control relies on the assumption that the dynamics can be perfectly estimated, it cannot be guaranteed to perform well when the dynamics are unknown [6]; this will be demonstrated in the control comparison section.

B. Sliding Mode Control

As mentioned previously, the primary feature of SMC is how the control switches sign to drive the state toward a sliding surface. The sliding surface is chosen such that while the state is on the surface, the dynamics of the surface will bring the state to the desired equilibrium; Moosavian et al. use an integral sliding surface as follows, which this paper uses as well [6, eqs. (22),(23)]:

$$\begin{aligned} s &= \dot{q} - \dot{q}_r \\ \dot{q}_r &= \dot{q}_d - K_d \tilde{q} - K_p \int_0^t \tilde{q}(\tau) d\tau \end{aligned} \tag{12}$$

where s is the sliding surface function and the other variables are all defined as in the previous section.

Note that if we differentiate (12) and then set $s = \dot{s} = 0$ as it ideally becomes when the state is on the sliding surface, the result is the same as (11), meaning the tracking error will converge to 0. It naturally follows that the control for this ideal case is the same as in (8).

The ideal case corresponds to exact knowledge of the dynamics [6]. In practice, the state will overshoot and pass through the sliding surface onto the other side. This can be avoided by choosing a switching controller:

$$\tau = -\hat{C}\dot{q} - \hat{G} + \hat{M}\ddot{q}_r - K\ \mathrm{sat}(s/\varepsilon) \tag{13}$$

where K is a diagonal positive gain matrix.

The function $\mathrm{sat}(s/\varepsilon)$ is a saturation function, defined as

$$\mathrm{sat}(s/\varepsilon) = \begin{cases} 1, & s/\varepsilon \geq 1 \\ s/\varepsilon, & |s|/\varepsilon < 1 \\ -1, & s/\varepsilon \leq -1 \end{cases} \tag{14}$$

where $\varepsilon > 0$ is called the boundary layer thickness [6] and regulates how often the controller switches to avoid undesirable chattering. Moosavian et al. note that a larger ε smooths out the control more but reduces the controller's robustness [6].

Moosavian et al. also prove that if one chooses Lyapunov function $V = s^\top M s$, then $\dot{V} < \eta s$ so long as [6, eqs. (27)-(30)]:

$$\begin{aligned} K_i &\geq \left| \tilde{M}\ddot{q}_r + \tilde{C}\dot{q}_r + \tilde{G} \right|_i + \eta_i \\ \eta_i &> 0 \end{aligned} \tag{15}$$

where $\tilde{M}, \tilde{C}$, and $\tilde{G}$ are the errors in parameter estimation.

Finally, Moosavian et al. introduce a way to regulate η to inprove the smoothness of the controller further [6, eqs. (33),(34)]:

$$\begin{aligned} \eta_i &= \frac{1}{2}\eta_{c,i}\left[(1-\sigma)\frac{\left|1-e^{|s|}\right|}{\left|1-e^{|\varepsilon|}\right|} + (1+\sigma)\right] \\ \sigma &= sgn\left(\frac{|s|}{\varepsilon} - 1\right) \end{aligned} \tag{16}$$

For the simulation, the chosen parameters are $\omega_n = 15$ rad/s, $\varepsilon = 0.5$, $\eta_{c,i} = 1$, and $K = \mathrm{diag}(21, 16, 5, 5)$.

A smaller ε caused the required gain to walk four steps to increase, so the gain and the boundary layer thickness were chosen by hand to balance having a small gain against having smooth control input with a minimum of chattering.

K was chosen by varying M, C, and G in simulation by 10% in either direction and approximately finding the maximum of the expression in (15).

IV. RESULTS AND COMPARISON

A. Reducing Ankle Torque

The first result for both controllers is their performance when all joint torques were allowed to grow as high as necessary. Figs. 2 and 3 show the tracking error and input torque of the CTM controller in this situation, respectively. In comparison, the performance of the SMC controller is shown in Figs. 4 and 5. The step time is 0.88s, so each plot shows 4 steps.

At the beginning of each step, the tracking error increases due to small mismatches introduced by the impact, but then decreases to near 0 before the next step. The periodicity of the output implies that the gait is stable or nearly stable and can continue for more steps than shown.

The maximum torque requirement for both controllers is just above 100 at the lowest gain, but the SMC's error is 10 times higher. However, once the ankle torque is saturated at an upper bound of 99 or less, the differences decrease. Figure 6 shows the error for the CTM controller when the ankle torque is saturated at 99. The SMC tracking error (not shown) looks the same but the error is 50% higher. The figure shows how once the ankle's ability to correct the trajectory is reduces, the error introduced in each step grows until the robot violates a constraint (such as in Figure 7 where its knee bends backwards) or it fails to complete a step at all.

Both controllers become unable to finish even a single step without violating the constraints when the upper bound on the ankle torque decreases to 95 or below. This reliance on ankle actuation shows why controllers for fully-actuated robots cannot be applied to underactuated robots, which need additional analysis.

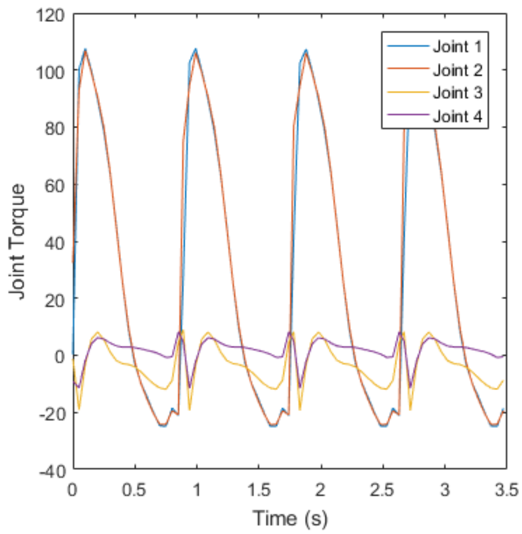

Fig. 2. Tracking error for CTM controller, no torque maximum.

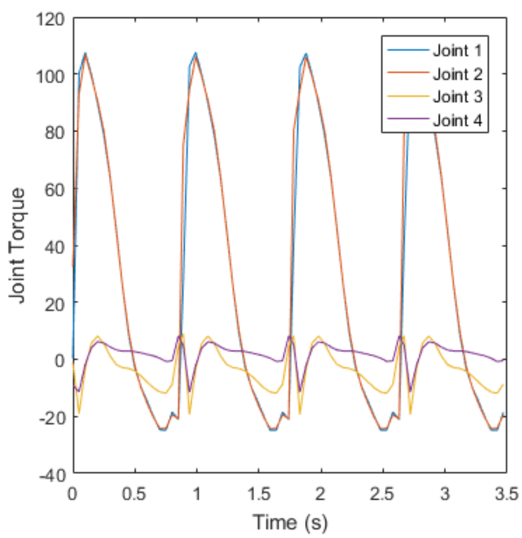

Fig. 3. Joint torque for CTM controller, no torque maximum.

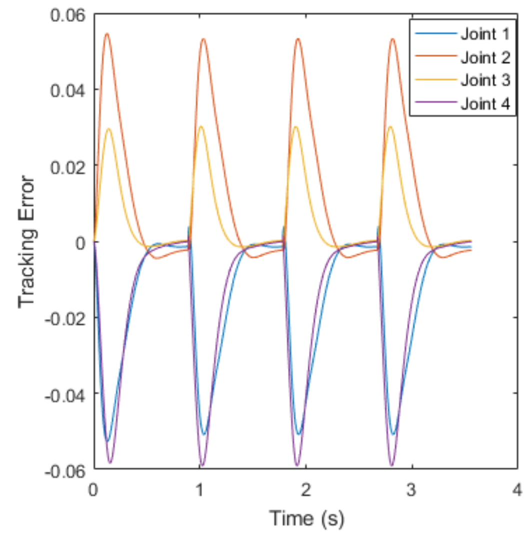

Fig. 4. Tracking error for SMC controller, no torque maximum.

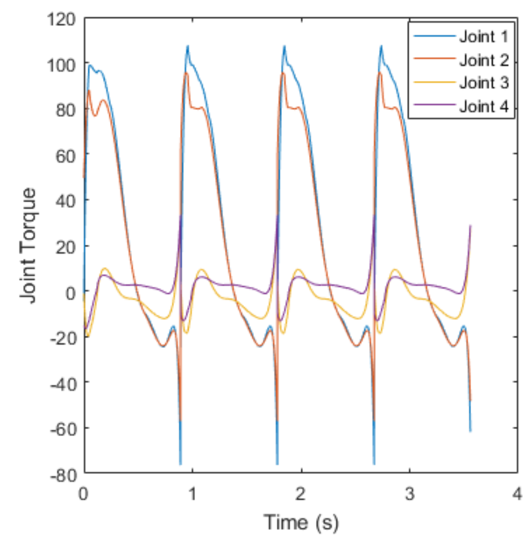

Fig. 5. Joint torque for SMC controller, no torque maximum.

Overall, the CTM controller appears to be better in terms of tracking error whenever the dynamics are known. However, as the next section will show, this is not the case when parameter uncertainty was introduced.

B. Parameter uncertainty

In this section of the evaluation, the torques are again allowed to grow as necessary. Now, the mass and other matrices are increased, then reduced by up to 10% of their nominal value. When all the parameters are reduced, both controllers track the trajectory for four steps. The maximum error for the CTM controller increases by 37% over the nominal value (Fig. 8), while the error of the SMC controller decreases by 68% from the nominal value (Fig. 9).

When the all the parameters increase by 10%, the CTM controller can only finish one step (Fig. 10), while the SMC controller can finish all four steps as shown in Fig. 11.

V. CONCLUSIONS

In this paper, a calculated torque method controller and a sliding mode controller were designed and implemented in a simulation of a fully actuated biped walker with knees. The results support the claims in the literature that underactuated systems cannot be reliably controlled by traditional controllers. The CTM tracking error was lower when the dynamics are known because of the relatively large boundary layer of the SMC controller; if the boundary layer is reduced, the SMC error can be made smaller. Overall, SMC is preferable to CTM because it is more robust in the face of significant parameter uncertainty, which is common in real-world robotics, and because chatter can be reduced by multiple methods. This finding is also in agreement with the existing literature. Future works planned include designing a higher order sliding mode controller that can control an

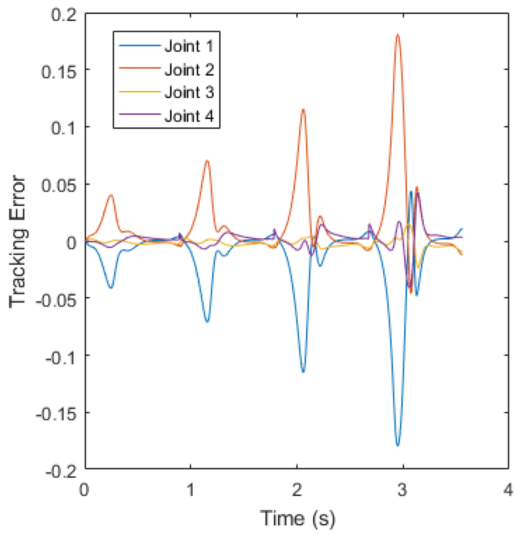

Fig. 6. Tracking error for CTM controller, Joint 1 limited to 99.

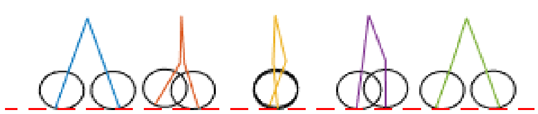

Fig. 7. A walking trajectory that violates human walking constraints.

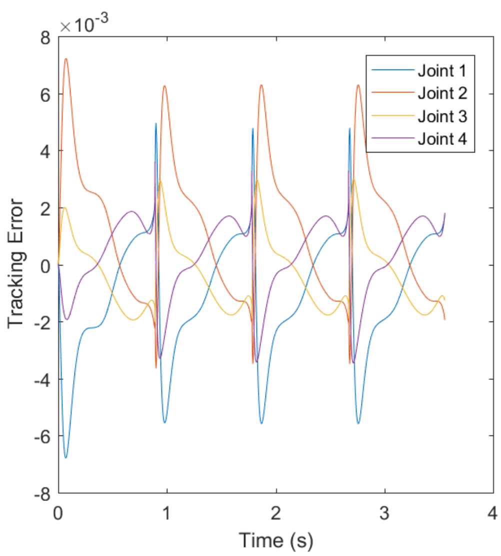

Fig. 8. Tracking error for CTM controller, parameters at 90% of nominal.

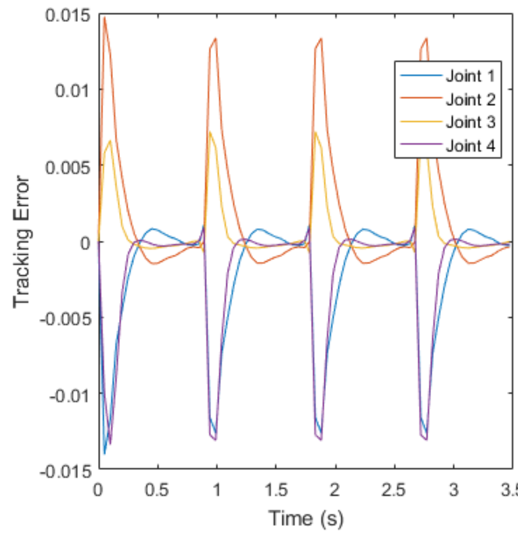

Fig. 9. Tracking error for SMC controller, parameters at 90% of nominal.

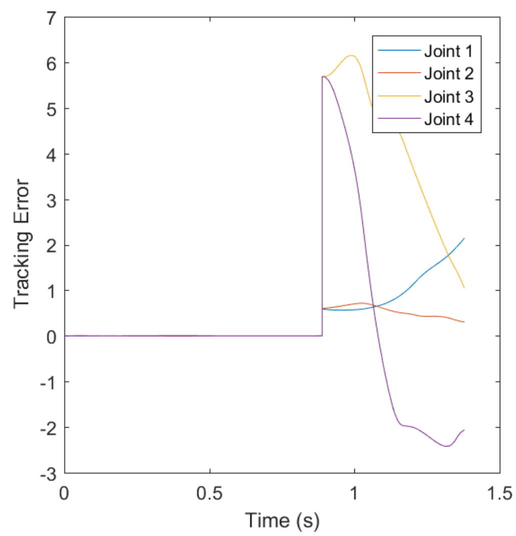

Fig. 10. Tracking error for CTM controller, parameters at 110% of nominal.

underactuated system, as well as the creation and analysis of a model that allows slipping between the feet and ground.

ACKNOWLEDGMENT

The author thanks Dr. Matthew Kelly for his trajectory optimization library for MATLAB. He also thanks Dr. Pilwon Hur for his advice during the modeling of the biped walker and for his impact calculations. In addition, the author is grateful to Kenneth Chao for the algorithm to approximate the trajectory and its derivatives by polynomials and for other insights, and Namita Kumar and Christian DeBuys for their insight and expertise throughout the research process.

REFERENCES

[1] S. Gupta and A. Kumar, "A brief review of dynamics and control of underactuated biped robots," Advanced Robotics, vol. 31, no. 12, pp. 607–623, April 2017. doi: 10.1080/01691864.2017.1308270

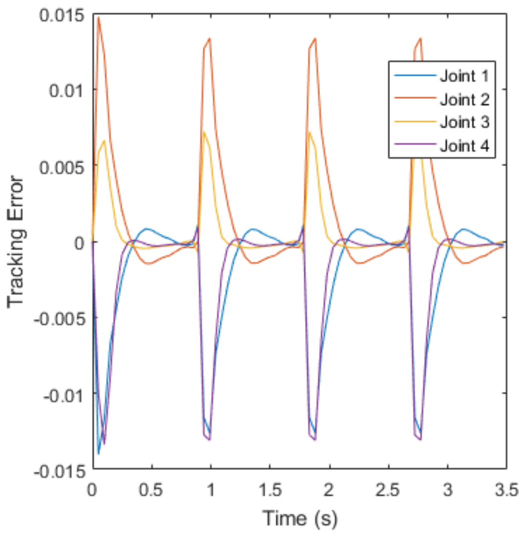

Fig. 11. Tracking error for SMC controller, parameters at 110% of nominal.

[2] T. McGeer, “Passive dynamic walking,” Int. J. Robotics Res., vol. 9, no. 2, pp. 62–82, April 1990.

[3] V. F. Hsu Chen, “Passive dynamic walking with knees: a point foot model,” M.S. thesis, Massachusetts Institute of Technology, Boston, MA, USA, February 2007.

[4] M. P. Kelly, OptimTraj. (2016) [Online]. Available: https://github.com/MatthewPeterKelly/OptimTraj, Accessed on: April 6, 2018.

[5] J. E. Slotine and W. Li, “Applied Nonlinear Control,” Prentice-Hall, Englewood Cliffs, New Jersey, 1991, pp. 211–212.

[6] S. A. A. Mossavian, A. Takhmar, and M. Alghooneh, “Regulated sliding mode control of a biped robot,” in *Proceedings of IEEE International Conference on Mechatronics and Automation*, 2007, pp. 1547–1552.

[7] Zhuang Lin, Qidan Zhu and Chengtao Cai, ”Variable Structure Control Based on Sliding Mode for a 2-DOF Underactuated Robot Manipulator,” *2006 6th World Congress on Intelligent Control and Automation*, Dalian, 2006, pp. 2029-2033.

[8] S. Mahjoub, F. Mnif and N. Derbel, ”A sliding mode control applied to whirling pendulum,” *2008 2nd International Conference on Signals, Circuits and Systems*, Monastir, 2008, pp. 1-6. doi: 10.1109/ICSCS.2008.4746910

[9] C. O. Saglam and K. Byl, “Stability and gait transition of the fivelink biped on stochastically rough terrain using a discrete set of sliding mode controllers.” *2013 IEEE International Conference on Robotics and Automation*. Karlsruhe; 2013. pp. 5675-?5682. doi: 10.1109/ICRA.2013.6631393.

[10] R. L. Huston, *Principles of Biomechanics*. Boca Raton: CRC Press, 2009.

[11] D. A. Winter, *Biomechanics and Motor Control of Human Movement*, 4th ed. Toronto: John Wiley & Sons, 2009.

[12] M. P. Kelly, “Transcription methods for trajectory optimization: a beginners tutorial,” arXiv:1707.00284 [math.OC], July 2017.